

COMPARISON OF THREE TIME-VARYING DELAY ESTIMATORS WITH APPLICATION TO ELECTROMYOGRAPHY

F. Leclerc¹⁻³, P. Ravier¹, O. Buttelli² and J.-C. Jouanin³

¹Laboratory of Electronics, Signals, Images, Polytech'Orléans - University of Orleans
12, rue de Blois, BP 6744 Cedex 2, F-45067 Orléans, France

²Activité Motrice et Conception Ergonomique - University of Orleans
Rue de Vendôme - BP 6237, F-45062 Orléans Cedex 2, France

³Institut de Médecine Aérospatiale du Service de Santé des Armées
BP 73, F-91223, Brétigny-sur-Orge Cedex, France

phone: + 33 1 69 23 79 79, fax: + 33 1 69 23 70 02, email: fleclerc@imassa.fr

ABSTRACT

It is known that the conduction velocity (CV) is a relevant estimator for fatigue and disease electromyographic (EMG) studies. CV estimation, which is linked to the time delay of an EMG signal propagation between two or more sensors, is particularly interesting in dynamic studies to detect local changes along the time. In this paper, we investigate three naturally time-frequency and time-scale methods to follow CV changes. In this work, the linear relationship between the phase information and the local time delay between two signals is used. Our results indicate that the three methods can be used to follow the conduction velocity evolution during a recording. Comparing the root mean square errors for each method highlight that the Fourier coherence method gives the best results compared to the two other methods (wavelet phase coherence and phase consistency).

1. INTRODUCTION

The problem of time delay estimation (TDE) is of interest in many applications such as sonar, radar, speech, seismology or electrophysiology. In surface electromyography (sEMG), the TDE permits to obtain the conduction velocity (CV) that is the speed of the electrical wave propagating along the muscle fiber direction. This indicator is considered as a relevant estimator to analyse the muscle property changes during a dynamic or isometric contraction [4, 5] and its evolution is useful in fatigue and neuromuscular diseases studies.

Basically, only two signals can be used to estimate the CV of the signal along the muscle fiber. Increasing the number of electrodes yields to reducing the variance of the estimate also allowing the estimation of the muscle fiber direction [8] in a matrix configuration case. The most popular sensor is composed of regularly and linearly spaced electrodes, for which the general model can be defined as:

$$x_k(t) = a_k(t)s(\alpha_k(t)t - (k-1)\theta(t)) + w_k(t) \quad (1)$$

$$k = 1, \dots, K; \quad 0 \leq t \leq T$$

where s is the original signal measured on K channels as $x_k(t)$. In this model, $\theta(t)$ is the time-varying delay between adjacent channels, $\alpha_k(t)$ is a scaling factor, $a_k(t)$ is a deformation factor, $w_k(t)$ is an independent identically distributed

(iid) Gaussian noise, k is the number of channel and T is the duration of the observation.

The estimation of a constant delay was intensively treated in the past [10, 6] in bioelectrical applications. In the sEMG basic investigations, the definition (1) is simplified: no scaling and deformation factors are introduced in the model and the delay is supposed to be constant within the window under interest. In this case, the equation 1 is rewritten as:

$$x_k(t) = s(t - (k-1)\theta) + w_k(t) \quad (2)$$

Based on this model, time or frequency estimation methods with two or more adjacent signals were used to estimate θ [6]. However, these methods assume signal stationarity and constant delay within an epoch of approximately 0.5 to 1 s. For shorter epochs (≤ 100 ms), only one maximum likelihood criterion algorithm has been proposed [7]. For nonstationary sEMG signals, natural time-frequency or time-scale methods can be used.

Within this scope, we selected three time-varying delay estimation methods and proposed an experimental set-up for their comparison. All these methods are based on the phase analysis in a transformed domain. Two of them used the Fourier transform [1] approach and one, the wavelet transform. To our knowledge, none of these methods have been tested for time-varying CV estimation.

In order to carry out the comparison, a sigmoidal CV evolution was created and used as possible evolution of the CV during an experimentation. The methods used to create test signals are presented in section 2. Section 3 describes the TDE algorithms. Section 4 presents the results and a discussion is given in section 5. Finally, some conclusions are drawn in the section 6.

2. SIGNAL DEFINITION AND TIME DELAY MODELING

In this study, we considered a reduced version of equation 1 with two channels:

$$\begin{aligned} x_1(t) &= s(t) + w_1(t) \\ x_2(t) &= s(t - \theta(t)) + w_2(t) \end{aligned} \quad (3)$$

2.1 Signal definitions

In TDE studies, $s(t)$ is classically assumed to be a white gaussian noise (WGN). This assumption is not a realistic one for sEMG signals. The sEMG signal is known to be

The work of F. Leclerc was financially supported by IMASSA Center.

limited in the 10-500 Hz frequency band. The generation of sEMG signals were performed using the model proposed in [3] where the low frequency f_l and the high frequency f_h are specified. The power spectral density of the modeled sEMG signal is given by:

$$P(f) = \frac{k f_h^4 f^2}{(f^2 + f_l^2)(f^2 + f_h^2)^2} \quad (4)$$

Using this model, we simulated temporal sEMG data by filtering a WGN with the inverse Fourier transform of the square root of $P(f)$. In this study, we used $f_l = 60$ Hz and $f_h = 120$ Hz. A 100-tap filter were retained.

In order to evaluate the applicability of different time varying estimation methods, we considered sEMG signals without noise.

2.2 Modeling time-varying delay

2.2.1 Delayed signal generation

To simulate the changes that can appear on the CV, we used the time delay modeling algorithm presented in [2]. This approach permits to create variable delays that are not necessarily linked to the temporal sampling step:

$$x_2(t) = \int_{-\infty}^{+\infty} \text{sinc}(\theta(t) + \tau) x_1(t - \tau) d\tau \quad (5)$$

where $\theta(t)$ is a time-varying delay function.

The signal $x_1(t)$ is generated according to 2.1 and $x_2(t)$ corresponds to the delayed version of $x_1(t)$. The sampled version of the equation 5 reads:

$$\tilde{x}_2(n) = \sum_{i=-p}^{p-1} \text{sinc}(\theta(n) + i) x_1(n - i) \quad (6)$$

where n is the sample number. The summation is made on the $2p$ coefficients of a finite order filter (the *sinc* function) leading to an approximation $\tilde{x}_2(n)$ of $x_2(n)$. In our simulations, p was fixed to 20.

2.2.2 Conduction velocity modeling

The CV evolution was modelised as a sigmoid function. This model combines possible physiological fast and slow changes during an experimentation. We expressed the CV function as:

$$CV(t) = \frac{5}{1 + e^{-\lambda(t-2.5)}} + 3 \quad (7)$$

where λ is linked to the slope of the sigmoid.

Based on a maximal acceleration of 2 m.s^{-2} , we found $\lambda = \frac{8}{5}$. Signals duration was 5 s with a CV range between 3 m.s^{-1} and 8 m.s^{-1} .

The time varying delay $\theta(t)$ is linked to the CV by the following formula:

$$\theta(t) = \frac{\Delta e}{CV(t)} \quad (8)$$

where Δe is the interelectrode distance ($\Delta e = 8 \text{ mm}$).

3. METHODS

3.1 Basic tools

Temporal approaches for time delay estimation are faced with temporal resolution linked to sampling frequency. The frequency approach solves this problem because it leads to a linear phase slope that is dependent of the temporal delay. In this approach, considering time-varying delays does not have obvious solutions. In order to test the ability of natural time-frequency or time-scale methods to follow temporal changes, we considered that the delays are locally constant. In this case, we will estimate the slope of the phase for each instant. The phase information is contained in the local cross-spectrum $P_{x_1 x_2}(t, f)$ and local cross-scalogram $W_{x_1 x_2}(t, a)$ respectively defined as:

$$\begin{aligned} P_{x_1 x_2}(t, f) &= X_1(t, f) X_2^*(t, f) = |P_{x_1 x_2}(t, f)| e^{i\phi_{x_1 x_2}(t, f)} \\ W_{x_1 x_2}(t, a) &= WT_1(t, a) WT_2^*(t, a) \end{aligned} \quad (9)$$

where the asterisk refers to the conjugate of the signal. $X_1(t, f)$ and $X_2(t, f)$ are the local Fourier transform of the signals $x_1(t)$ and $x_2(t)$, $WT_1(t, a)$ and $WT_2(t, a)$ are the continuous wavelet transform of the same signals:

$$\begin{aligned} X_i(t, f) &= \int_{-\infty}^{+\infty} h(\tau - t) x_i(\tau) e^{-i2\pi f \tau} d\tau \\ WT_i(t, a) &= \int_{-\infty}^{+\infty} x_i(\tau) \frac{1}{\sqrt{a}} \psi^*\left(\frac{\tau - t}{a}\right) d\tau \end{aligned} \quad (10)$$

where $h(t)$ is the Hanning weighting window function restricting the Fourier transform around a time instant t . The function ψ is the parameterized complex Morlet wavelet [11], for which the central frequency f_0 and the bandwidth (*i.e* the duration of the mother wavelet) can be specified. The frequency f is linked to the scale a and to f_0 by the relation $f = \frac{f_0}{a}$. Thus, we can consider $WT_i(t, a)$ as a function of f and $W_i(t, a)$ will be rewritten as $W_i(t, f)$.

Since the data are random, the equations 10 have to be expressed with a mathematical expectation. In the following sections, the latter formulas will be redefined with averaging estimations.

3.2 Fourier phase coherency

Coherence is a measure of linear predictability [10]: 0 if the signals are not linearly related, 1 if they are. This information will be used to select frequencies of interest by comparing the coherence of each frequency to a specific threshold (0.995). In the following methods, we will thus present normalized estimations, even if the denominator part brings no phase information.

The local Fourier coherence of two signals $x_1(t)$, $x_2(t)$ is defined as:

$$\text{coh}F_{x_1 x_2}(t, f) = \frac{E_t\{P_{x_1 x_2}(t, f)\}}{\sqrt{E_t\{P_{x_1 x_1}(t, f)\}} \sqrt{E_t\{P_{x_2 x_2}(t, f)\}}} \quad (11)$$

The expectations were estimated by the Welch method. Each N -sample window was divided in three $N/2$ -samples Hanning weighted windows with 50% of overlapping.

$cohF_{x_1x_2}(t, f)$ is a complex time-frequency plane where the phase can be easily extracted at each instant. Indeed, only the numerator lead to a phase term since 3 and 11 lead to $E_t\{P_{x_1x_2}(t, f)\} = E_t\{S(t, f)S^*(t, f)\}e^{2i\pi\theta f}$, where $S(t, f)$ is the Fourier transform of $s(t)$ and θ is considered as locally constant. Practically, estimation of θ is carried out by a linear regression on the phase $\Phi_F(t, f)$, in least square sense.

3.3 Phase consistency

The local cross-spectrum can be differently averaged in time as [1]:

$$\begin{aligned} \kappa_{x_1x_2}(t, f) &= E_t\left\{\frac{P_{x_1x_2}(t, f)}{\sqrt{P_{x_1x_1}(t, f)}\sqrt{P_{x_2x_2}(t, f)}}\right\} \\ &= E_t\{e^{i\phi_{x_1x_2}(t, f)}\} \end{aligned} \quad (12)$$

In this definition, we estimate an averaged local normalized cross-spectrum by averaging 20 ms of normalized cross-spectra around an instant t . By analogy with the method described in the section 3.2, the delay was estimated at each instant by a linear regression on the phase of $\kappa_{x_1x_2}(t, f)$.

3.4 Wavelet phase coherency

The local wavelet coherence of two signals $x_1(t), x_2(t)$ can be defined as:

$$cohW_{x_1x_2}(t, f) = \frac{E_t\{W_{x_1x_2}(t, f)\}}{\sqrt{E_t\{W_{x_1x_1}(t, f)\}}\sqrt{E_t\{W_{x_2x_2}(t, f)\}}} \quad (13)$$

The formula 13 was estimated by δ -sample averaging where δ is linked to the frequency f by $\delta(f) = percentage \cdot f_0/f$. We chose $percentage = 0.05$ which corresponds to a 50 ms averaging of $cohW_{x_1x_2}(t, f)$ at the frequency $f = f_0 = 60Hz$.

Similarly to 3.2, the delay is embedded in the phase information since $\Phi_W(t, f) = 2\pi f\theta$.

4. RESULTS

In this section, the three time delay estimators described above are compared *via* simulation studies. An example of the sigmoid CV function with the corresponding estimated CV is given in figure 1. The variance is high whenever the slope is steep as well as for large CV values since CV estimation errors are inversely proportional to square delay estimation errors.

Monte-Carlo simulations with 100 independent runs were performed. We considered window analysis durations between 0.125 s to 1 s. Standard deviation and bias values were numerically calculated for the three estimation methods considering, in practice, windows of 128-256-512-1024 samples at a frequency rate $F_s = 1024Hz$.

Results of the local coherence phase algorithm are presented on the figure 2.

On this figure, the bias was negative for windows of duration 1s and 0.5s and was positive for shorter windows (0.125s and 0.25s). Standard deviation was minimum for a window duration of 0.25s.

Results of the phase consistency algorithm are presented on the figure 3.

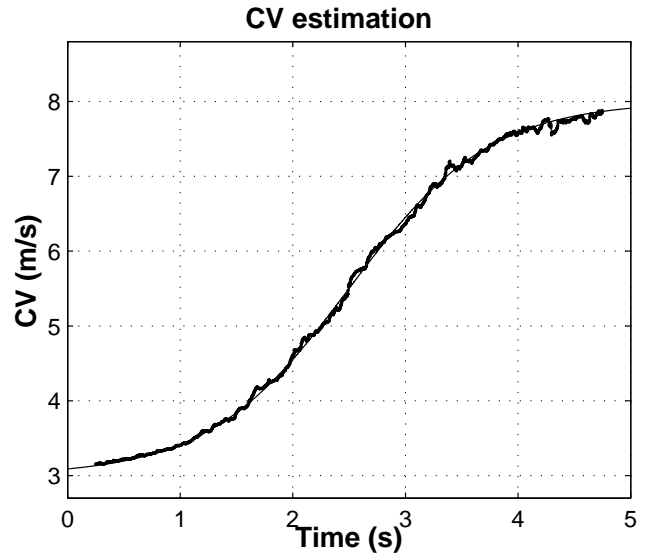


Figure 1: Example of CV estimation with the Fourier coherence phase method.

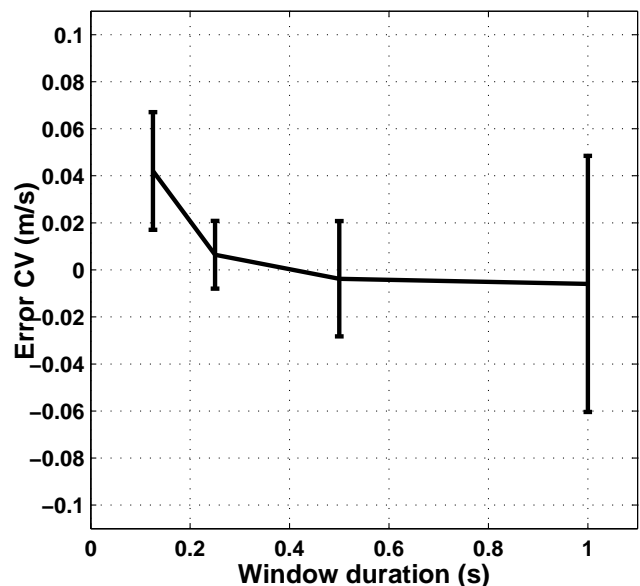


Figure 2: Estimation results using Fourier phase coherence estimator. Bias and standard deviation are reported as a function of the four window durations, 0.125s, 0.25s, 0.5s, 1s.

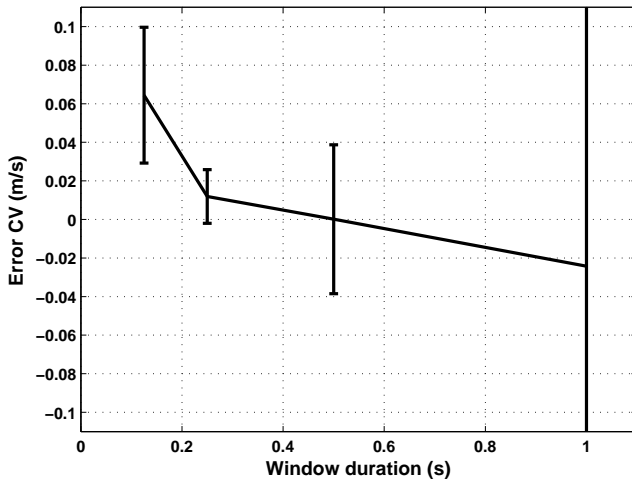


Figure 3: Estimation results using phase consistency estimator. Bias and standard deviation are reported as a function of the four window durations, 0.125s, 0.25s, 0.5s, 1s.

The trend of the results for the phase consistency estimation was similar to the results found with the Fourier coherence phase algorithm. Excepted for the 0.25s duration window, the standard deviation of the phase consistency estimator is more important.

Results of the wavelet phase coherence algorithm are presented on the figure 4. The bias is always positive. The standard deviation are less good than the preceding methods even if it appears to be less sensitive than the other methods in a wide range of mother wavelet durations (between 0.5s and 1.5s).

5. DISCUSSION

As expected, a compromise between the duration of the analysis window and the speed of CV variation exist. The results suggest that, in a physiological point of view, the analysis duration should be at least 0.25s. Shorter periods will increase the estimation error. Longer periods can be chosen depending on the dynamic character of the experiment. Recall that our CV sigmoid function contains the fastest variations of physiological CV that could be observed.

Results obtained with time-scale approach seem to be disappointing. However, our chosen parameters are certainly not optimized and other wavelet coefficient averaging techniques can be investigated. The observed bias is not really disturbing in a physiological sense since trends are usually analysed.

6. CONCLUSION

The concern of this article was to estimate the ability of natural time-frequency and time-scale methods to follow time-varying delays on band limited signals. Application of these algorithms was the estimation of the conduction velocity of electromyographic signals. sEMG signal, free of noise, were simulated to test the algorithms. This study has now to be carried out including noisy observations. The tested algorithms also have to be applied on real experimental data.

In this study, we focused on using the phase information of time-frequency and time-scale transforms. Of course, the

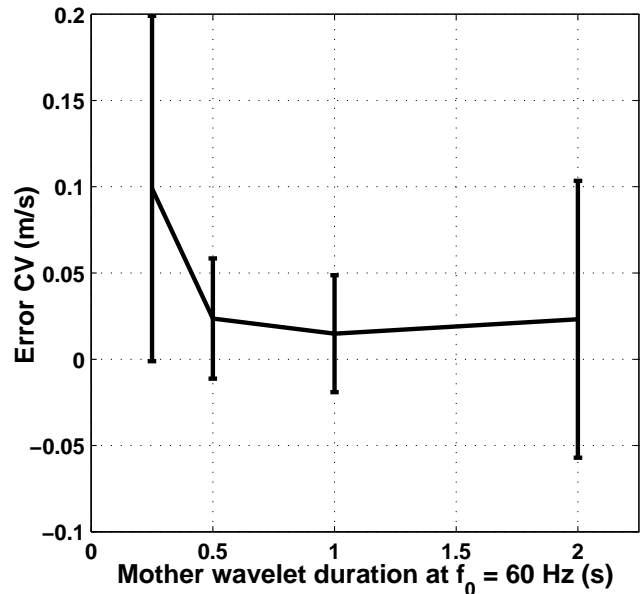


Figure 4: Estimation results using wavelet phase coherence estimator. Bias and standard deviation are reported as a function of the four mother wavelet duration defined at the central frequency $f_0=60$ Hz, 0.25s, 0.5s, 1s, 2s. The duration of the wavelet is defined as its standard deviation.

problem of TDE estimation can be solved differently:

- searching the delays can be processed in the Maximum Likelihood Estimation sense with optimization techniques and objective functions [10].
- the chosen methods belong to the larger classes of affine class and Cohen's class. Many other transforms in this frame could have been studied involving different kinds of weighting functions in the time and/or frequency domains, also introducing the delicate problem concerning the choice of their related parameters.

This study is a first step in the time-varying CV estimation problem. Future works concern the introduction of time-varying delays in the time-frequency/time-scale methods. A theoretical derivation can be found considering a first order expansion of the time-varying delay.

REFERENCES

- [1] A. Bruns, "Fourier-, Hilbert- and wavelet-based signal analysis: are they really different approaches?," *Journal of Neuroscience Methods*, vol. 135, pp. 321-332, 2004.
- [2] Y. Chan, J. Riley and J. Plant, "Modeling of time delay and its application to estimation of nonstationary delays," *IEEE Transactions on Acoustics, Speech, and Signal Processing* [see also *IEEE Transactions on Signal Processing*], vol. 29, pp. 577-581, 1981.
- [3] D. Farina and R. Merletti, "Comparison of algorithms for estimation of EMG variables during voluntary isometric contractions," *J Electromyogr Kinesiol*, vol. 10, pp. 337-349, 2000.
- [4] D. Farina, L. Arendt-Nielsen, R. Merletti and T. Graven-Nielsen, "Assessment of single motor unit conduction velocity during sustained contractions of the tibialis an-

terior muscle with advanced spike triggered averaging,” *Journal of Neuroscience Methods*, vol. 115, pp. 1-12, 2002.

- [5] D. Farina, M. Gazzoni and R. Merletti, “Assessment of low back muscle fatigue by surface EMG signal analysis: methodological aspects,” *Journal of Electromyography and Kinesiology*, vol. 13, pp. 319-332, 2003.
- [6] D. Farina and R. Merletti, “Methods for estimating muscle fibre conduction velocity from surface electromyographic signals,” *Medical and Biological Engineering and Computing*, vol. 42, pp. 432-44, 2004.
- [7] D. Farina, M. Pozzo, E. Merlo, A. Bottin and R. Merletti, “Assessment of average muscle fiber conduction velocity from surface EMG signals during fatiguing dynamic contractions,” *IEEE Transactions on Biomedical Engineering*, vol. 51, pp. 1383-1393, 2004.
- [8] C. Grönlund, N. Ostlund, K. Roeleveld, J.S. Karlsson, “Simultaneous estimation of muscle fibre conduction velocity and muscle fibre orientation using 2D multichannel surface electromyogram,” *Med Biol Eng Comput*, vol. 43, pp. 63-70, 2005.
- [9] E. Merlo, M. Pozzo, G. Antonutto, P. E. di Prampero, R. Merletti and D. Farina, “Time-frequency analysis and estimation of muscle fiber conduction velocity from surface EMG signals during explosive dynamic contractions,” *Journal of Neuroscience Methods*, vol. 142, pp. 267-274, 2005.
- [10] T. Müller, M. Lauk, M. Reinhard, A. Hetzel, C. H. Lücking and J. Timmer, “Estimation of delay times in biological systems,” *Ann Biomed Eng*, vol. 31, pp. 1423-1439, 2003.
- [11] A. Teolis, *Computational signal processing with wavelets*, Birkhauser ,1998.